

Reversible Ligand-Induced Dissociation of a Tryptophan-Shift Mutant of Phosphofructokinase from *Bacillus stearothermophilus*^{†,‡}

Michelle R. Riley-Lovingshimer,^{§,||} Donald R. Ronning,^{§,⊥} James C. Sacchettini,[§] and Gregory D. Reinhart^{*,§,||}

Department of Biochemistry and Biophysics and Center for Advanced Biomolecular Research, Texas A&M University, 2128 TAMU, College Station, Texas 77843-2128

Received June 22, 2002; Revised Manuscript Received August 28, 2002

ABSTRACT: The biophysical properties of a tryptophan-shifted mutant of phosphofructokinase from *Bacillus stearothermophilus* (BsPFK) have been examined. The mutant, designated W179Y/Y164W, has kinetic and thermodynamic properties similar to the wild-type enzyme. A 2-fold decrease in k_{cat} is observed, and the mutant displays a 3-fold smaller $K_{0.5}$ for the substrate, fructose-6-phosphate (Fru-6-P), as compared to the wild-type enzyme. The dissociation constant for the inhibitor, phospho(enol)pyruvate (PEP), increases 2-fold, and the coupling parameter, Q_{ay} , decreases 2-fold. This suggests that while the mutant displays a slightly decreased affinity for PEP, PEP is still an effective inhibitor once bound. The new position of the tryptophan in W179Y/Y164W is approximately 6 Å from the Fru-6-P portion of the active site. A 25% decrease in fluorescence intensity is observed upon Fru-6-P binding, and an 80% decrease in fluorescence intensity is observed with PEP binding. In addition, the intrinsic fluorescence polarization increases from 0.327 ± 0.001 to 0.353 ± 0.001 upon Fru-6-P binding, but decreases to 0.290 ± 0.001 when PEP binds. Most notably, the presence of PEP induces dissociation of the tetramer. Dissociation of the tetramer into dimers occurs along the active site interface and can be monitored by the loss in activity or the loss in tryptophan fluorescence that is observed when the enzyme is titrated with PEP. Activity can be protected or recovered by incubating the enzyme with Fru-6-P. Recovery of activity is enzyme concentration dependent, and the rate constant for association is $6.2 \pm 0.3 \text{ M}^{-1} \text{ s}^{-1}$. Ultracentrifugation experiments revealed that in the absence of PEP the mutant enzyme exists in an equilibrium between the dimer and tetramer forms with a dissociation constant of $11.8 \pm 0.5 \mu\text{M}$, while in the presence of PEP the enzyme exists in equilibrium between the dimer and monomer forms with a dissociation constant of $7.5 \pm 0.02 \mu\text{M}$. A 3.1 Å crystal structure of the mutant enzyme suggests that the amino acid substitutions have not dramatically altered the tertiary structure of the enzyme. While it is clear that wild-type BsPFK exists as a tetramer under these same conditions, these results suggest that quaternary structural changes probably play an important role in allosteric communication.

Phosphofructokinase (PFK)¹ has been purified to homogeneity from many sources and in some cases extensively studied as a model system of allosteric regulation (*1*). From mammalian to bacterial sources, all PFKs are oligomeric enzymes, and for most, the smallest active form of the enzyme is a tetramer (*2–5*). One interesting feature of allosteric enzymes in general is that in many cases the binding sites, either active or allosteric, lie along subunit interfaces. This requires that the enzyme be in its native oligomeric arrangement for catalytic activity and/or allosteric control

(*6*). Since the first purification of rabbit muscle PFK, Ling et al. (*7*) established that rabbit muscle PFK can exist as higher molecular weight aggregates that retain activity. Aggregation was thought to occur at the high enzyme concentrations that were required for physical measurement of the oligomeric state but not under the more dilute conditions of kinetic assay or even under physiological conditions. However, Reinhart and Lardy (*8–10*) showed that under physiological conditions, rat liver PFK does undergo higher order polymerization which is modulated by the presence of substrates and effectors. Furthermore, changes in the aggregation state of the protein in response to ligand binding have physiological ramifications. While association–dissociation equilibria appear to play an important role in the regulation of mammalian PFKs, the only bacterial PFK, observed to date, that undergoes changes in oligomeric structure as a result of ligand binding is *Thermus thermophilus* PFK (TtPFK) (*4*). However, the physiological relevance of ligand-induced dissociation of TtPFK has not been investigated.

Like most bacterial PFKs, TtPFK is a tetramer in its native state. However, TtPFK undergoes reversible dissociation to inactive dimers as a result of binding phospho(enol)pyruvate (PEP) in the allosteric site (*4*). While TtPFK has not been

[†] This work was supported by National Institutes of Health Grant GM33216 and Robert A. Welch Grant A-1543.

[‡] Coordinates for the structure of W179Y/Y164W BsPFK have been deposited in the Protein DataBank, accession number 1MTO.

* To whom correspondence should be addressed. E-mail: gdr@tam.u.edu.

[§] Department of Biochemistry and Biophysics.

^{||} Center for Advanced Biomolecular Research.

[⊥] Present address: Laboratory of Molecular Biology, National Institute of Diabetes and Digestive and Kidney Diseases, National Institutes of Health, Bethesda, MD 20892.

¹ Abbreviations: PFK, phosphofructokinase; TtPFK, phosphofructokinase from *Thermus thermophilus*; EcPFK, phosphofructokinase from *E. coli*; BsPFK, phosphofructokinase from *Bacillus stearothermophilus*; Fru-6-P, fructose-6-phosphate; PEP, phospho(enol)pyruvate; MOPS, 3-(*N*-morpholino)propanesulfonic acid.

as extensively studied as *E. coli* PFK (EcPFK) or *B. stearothermophilus* PFK (BsPFK), these enzymes are quite homologous. TtPFK is 57% identical to BsPFK and 47% identical to EcPFK (11). Even though reversible dissociation as a result of effector binding has not been reported in other bacterial PFKs, it has been hypothesized that effector binding to some allosteric enzymes causes quaternary structural changes that destabilize subunit interfaces without necessarily promoting changes in oligomeric structure (12). Therefore, by introducing a destabilizing mutation along the interface, one might alter the enzymatic response to effector binding such that the interface destabilization will be exaggerated compared to the wild-type enzyme and result in a modified oligomeric arrangement.

Both EcPFK and BsPFK have a single tryptophan per subunit. In the case of EcPFK, the tryptophan fluorescence is sensitive to local changes in the environment associated with ligand binding. The fluorescence changes have been utilized to examine ligand binding and allosteric interactions of EcPFK in the absence of turnover (13, 14). However, the tryptophan fluorescence of BsPFK does not exhibit analogous perturbations associated with ligand binding (15, 16). One strategy we have employed previously to circumvent this lack of fluorescence responsiveness has been to create tryptophan-shifted mutants of BsPFK in which the tryptophan has been removed from its native position and placed in alternative regions of the protein (16). The work presented in this study describes the unique properties of a second tryptophan-shifted mutant of BsPFK, designated "W179Y/Y164W".

The active site and the allosteric site of BsPFK are composed of residues from two adjacent subunits (6). The substrate, fructose-6-phosphate (Fru-6-P), binds between the subunits related by the *r*-axis dyad, which is referred to as the "active site" interface. The allosteric ligands bind in a cleft between subunits related by the *p*-axis dyad, which is referred to as the "allosteric site" interface. Tyr164 is positioned approximately 6 Å from Fru-6-P bound in the active site. Although it is in close proximity to the active site, Tyr164 does not appear to be directly involved in Fru-6-P binding (6). Changing this residue to a tryptophan results in an active enzyme with a slightly compromised specific activity. The experiments described here show that W179Y/Y164W dissociates into inactive dimers in the presence of PEP and that dissociation is reversible in the presence of Fru-6-P.

MATERIALS AND METHODS

Materials. All chemical reagents used in buffers, protein purifications, and fluorescence and enzymatic assays were of analytical grade, purchased from Sigma, Fisher, or Aldrich. The Matrex Gel Blue A-agarose resin for affinity chromatography was purchased from Amicon Corp. The coupling enzymes aldolase, triosephosphate isomerase, and glycerol-3-phosphate dehydrogenase in ammonium sulfate suspensions were purchased from Boehringer Mannheim. The coupling enzymes were dialyzed extensively against MOPS storage buffer (50 mM MOPS-KOH, pH 7.0, 100 mM KCl, 5 mM MgCl₂, 0.1 mM EDTA) before use. Creatine phosphate, creatine kinase, and sodium salts of Fru-6-P, ATP, and PEP were purchased from Sigma. Site-directed mutagenesis was carried out using the Altered Sites In Vitro

Mutagenesis System which was purchased from Promega. The system included pALTER-1 vector and pALTER-control vector, and the ampicillin repair and control oligonucleotides. Other oligonucleotides were synthesized using an Applied Biosystems 392 DNA/RNA synthesizer at the Gene Technologies Laboratory at the Institute of Developmental and Molecular Biology at Texas A&M University. Glycerol stocks of *E. coli* strains JM109, XL1-Blue, and BMH 71-18 *mutS* were purchased from either Promega or Stratagene. DF1020² cells were obtained from Dr. Robert Kemp (Chicago Medical School). DNA modifying enzymes and restriction endonucleases were purchased from either New England Biolabs or Promega. Deionized-distilled water was used throughout.

The oligonucleotides used to make the tryptophan-shifted mutant described in this study are complementary to the coding strand and listed below. Each mutation required a two-base substitution either to change the tryptophan to a tyrosine or to change the tyrosine to a tryptophan. The underlined bases indicate the triplet codon for the new amino acid in that position: W179Y, GC-CAG-CCC-CGA-ATA-TAA-GGC-GAT-GTC-GCC; Y164W, GCC-CAT-CAC-TTC-GAT-GAC-CCA-CGT-CCG-CTC-GTG-CG.

Site-Directed Mutagenesis. Site-directed mutagenesis was carried out using the Altered Sites In Vitro Mutagenesis System (Promega) and has previously been described (16). Wild-type and W179Y/Y164W PFKs were expressed in DF1020 (*garB10*, *fluA22*, *ompF627*(T₂^R), Δ *pfkB201*, *fad701*(T₂^R), *recA56*, *relA1*, *pit-10*, *spoT1*, Δ (*rhaD-pfkA*)200, *rrnB-2*, *mcrB1*, *cre510*) cells as described previously (16).

Protein Purification. Purification of wild-type and mutant BsPFKs was carried out as described by Riley-Lovingshimer and Reinhart (16). The only difference noted was that during the purification of W179Y/Y164W BsPFK there was no activity present in the crude extract. However, activity recovered to normal levels following the heat step. Although this observation was not extensively examined, we hypothesize based on subsequent investigations that the enzyme is in an inactive dimer form following cell lysis and reassociates to an active tetramer during the 70 °C incubation.

Protein Determination. Protein concentrations were determined by using the BCA protein assay reagent (Pierce) or by absorbance at 280 nm using an ϵ_{280} equal to 18 910 M⁻¹ cm⁻¹. ϵ_{280} was calculated based on the number of tryptophan and tyrosine residues (17). The concentrations calculated by both methods agreed well with one another.

Enzymatic Activity. BsPFK assays were performed using the coupled enzyme assay in which the production of fructose-1,6-bisphosphate leads to the oxidation of NADH (18, 19). Activity measurements were carried out in a 1.0 mL reaction volume containing 50 mM MOPS-KOH, 100 mM KCl, 5 mM MgCl₂, 0.1 mM EDTA, 2 mM DTT, 0.2 mM NADH, 3 mM MgATP, 250 μ g of aldolase, 50 μ g of glycerol-3-phosphate dehydrogenase, and 5 μ g of triosephosphate isomerase that was adjusted to pH 7.0. The concentrations for Fru-6-P and PEP were varied as indicated. Creatine kinase and creatine phosphate were added as an ATP regenerating system to avoid accumulation of ADP.

² The genotype given for *E. coli* strain DF1020 that was described in ref 16 is incomplete. Here we provide the complete genotype which was obtained from the *E. coli* Genetic Stock Center (Yale University).

Assays were initiated by the addition of 10 μL of BsPFK that had been appropriately diluted. Activity measurements were conducted on a Beckman Series 600 spectrophotometer using a linear regression calculation to convert the change in absorbance at 340 nm to enzyme activity. One unit of activity is defined as the production of 1 μmol of fructose-1,6-bisphosphate per minute.

Steady-State Fluorescence. Steady-state fluorescence intensity and polarization were measured using an SLM-4800 upgraded with electronics and software obtained from I. S. S. Inc. (Urbana, IL). Samples were excited using a xenon arc lamp and a monochromator to select for 300 nm light. Fluorescence intensity was detected either through an emission monochromator or through a 2 mm thick Schott WG-345 cut-on filter. To measure polarization, excitation and emission polarizers were placed in the appropriate positions, and emission was detected through a 2 mm thick Schott WG-345 cut-on filter. All titrations were carried out in MOPS storage buffer containing 1–5 μM enzyme. Titrations of W179Y/Y164W BsPFK with Fru-6-P or PEP were carried out in a 2 mL initial volume in a standard 1×1 cm cuvette. All measurements were blank-subtracted. Spectral or intensity measurements were also corrected for dilution of the protein.

Data Analysis. Data pertaining to the coupling for Fru-6-P and PEP obtained from kinetic assays were analyzed with a Power Macintosh 7100/80AV using Kaleidagraph 3.08 (Synergy Software) to fit to the following equations. The concentration of Fru-6-P which resulted in half-maximal activity, $K_{0.5}$, was determined using the Hill equation (20):

$$\frac{v}{[E]_t} = \frac{k_{\text{cat}}[A]^{n_H}}{(K_{0.5})^{n_H} + [A]^{n_H}} \quad (1)$$

where v is the steady-state rate of turnover, E_t is the total amount of enzyme active sites, and n_H is the Hill coefficient. The variation in $K_{0.5}$ as a function of PEP concentration was fit to the equation:

$$K_{0.5} = K_{\text{ia}}^o \left[\frac{K_{\text{iy}}^o + [Y]}{K_{\text{iy}}^o + Q_{\text{ay}}[Y]} \right] \quad (2)$$

where $K_{0.5}$ is the concentration of Fru-6-P resulting in half-maximal activity obtained from fitting to eq 1, Y represents PEP, K_{ia}^o is the dissociation constant for the substrate, Fru-6-P, in the absence of allosteric ligand, K_{iy}^o is the dissociation constant for the allosteric ligand, PEP, in the absence of substrate, and Q_{ay} is equal to the coupling parameter describing the extent to which the binding of the allosteric ligand effects the binding of substrate and vice versa as defined by the expression:

$$\frac{K_{\text{ia}}^o}{K_{\text{ia}}^\infty} = \frac{K_{\text{iy}}^o}{K_{\text{iy}}^\infty} = Q_{\text{ay}} \quad (3)$$

where K_{ia}^∞ and K_{iy}^∞ are the dissociation constants for A and Y, respectively, in the saturating presence of the other ligand. To be consistent with previously described conventions (13, 14, 16, 21–23), A represents Fru-6-P and Y represents PEP. By resolving both terms K_{iy}^o and Q_{ay} , eq 2 allows separate quantification of both effector binding affinity and its action once bound, respectively.

Data collected using fluorescence assays were analyzed using the following equation that is analogous to eq 1:

$$F = \frac{\Delta F[A]^{n_H}}{K_{0.5}^{n_H} + [A]^{n_H}} + F_o \quad (4)$$

where F is the steady-state fluorescence emission, F_o is equal to F when $[A] = 0$, and ΔF is equal to the limiting value of $F - F_o$ when $[A]$ is saturating.

Reactivation Experiments. Indicated concentrations of W179Y/Y164W BsPFK were incubated either in the absence of PEP or with 0.1 mM PEP. Samples in the absence of PEP were used to monitor changes in PFK activity that might occur over the time course of the experiment that are not related to PEP binding. For samples which included PEP, activity was monitored until complete loss of activity was observed. Fru-6-P was added to each sample to a concentration of 1 mM. Activities of both the control and PEP-incubated samples were monitored over time. The activity of control samples did not vary greatly over the course of the experiment, so the values were averaged and used as 100% activity. For PEP-incubated samples, the recovered activity was plotted as a function of time. In these experiments, it is presumed that PEP causes the enzyme to dissociate into inactive dimers and upon incubation with Fru-6-P active tetramers are recovered in accordance with the increase in enzyme activity. Therefore, reactivation is dependent upon enzyme concentration and a second-order process. Replotting the data as reciprocal inactive dimer (μM^{-1}) (calculated based on the known enzyme concentration and activity measurement) versus time results in a linear relationship, and the rate constant for the dimer to tetramer association can be obtained from the slope of the line.

Ultracentrifugation. Ultracentrifugation was carried out using a Beckman model XL-A ultracentrifuge at 20 °C. Enzyme monomer concentration was between 25 and 35 μM . Before centrifugation, enzyme was dialyzed into MOPS buffer with the addition of either 1 mM Fru-6-P, 1 mM PEP, or 1 mM of both ligands. For samples that included both ligands, the enzyme was first dialyzed with PEP to promote dimer formation. After 30 min, 1 mM Fru-6-P was added to initiate reassociation. Samples incubated with Fru-6-P were centrifuged at 10 000 rpm, and samples that were incubated with only PEP were centrifuged at 18 000 rpm. Samples were assumed to be at equilibrium when consecutive scans of the radial position at 280 nm taken at 2 h intervals were identical. Data used for analysis were the average of 20 successive scans. Absorbance values as a function of radial position were fit using Kaleidagraph 3.08 (Synergy Software) to either eq 5, which describes sedimentation of a single species, or eq 6, which describes sedimentation of a self-associating species (24–26).

$$A_r = \exp[\ln A_o + HM(r^2 - r_o^2) + C] \quad (5)$$

$$A_r = \exp[\ln A_o + HM(r^2 - r_o^2)] + \exp[\ln A_o^N + \ln(K_a)HNM(r^2 - r_o^2)] + C \quad (6)$$

$$H = \frac{(1 - \bar{v}\rho)\omega^2}{2RT} \quad (7)$$

Table 1: Thermodynamic and Kinetic Parameters for Wild-Type, W179F/F230W,^a and W179Y/Y164W Using both Kinetic and Fluorescence Assays

	k_{cat} (s ⁻¹)	K_{ia}° (μM)	K_{iy}° (μM)	Q_{ay} ($\times 100$)
wild-type ^b	95	25.3 \pm 0.5	16.6 \pm 0.4	0.84 \pm 0.02
W179F/F230W ^b	96	29.1 \pm 0.7	11.4 \pm 0.4	0.22 \pm 0.01
W179F/F230W ^c	N/A ^d	2.71 \pm 0.04	0.92 \pm 0.02	0.17 \pm 0.04
W179Y/Y164W ^b	45	8.4 \pm 1.5	30.8 \pm 8.0	0.37 \pm 0.09
W179Y/Y164W ^c	N/A ^d	0.11 \pm 0.04	9.2 \pm 2.6	0.27 \pm 0.09

^a Described previously (16). ^b Kinetic assays with MgATP concentration held constant at 3 mM. ^c Fluorescence assays. ^d Not applicable.

The terms in eqs 5 through 7 are defined as follows: A_r , the absorbance at radial position r ; A_{r_0} , the absorbance at a reference radius r_0 ; M , monomer molecular weight; N , the stoichiometry of association; K_a , the association constant; C , the baseline offset; \bar{v} , the partial specific volume (calculated to be 0.723 based on the amino acid composition of BsPFK); ρ , the buffer density; ω , the angular velocity in radians per second; R , the gas constant; and T , the temperature in degrees kelvin.

Crystallization of W179Y/Y164W BsPFK. In an effort to grow diffraction-quality crystals of W179Y/Y164W, a sparse matrix crystallization screening kit (Hampton Research, Laguna Hills, CA) was used. The conditions that produced crystals during the initial screen were 18% poly(ethylene glycol) (PEG) 8000, 0.1 M sodium cacodylate, pH 6.5, and 0.2 M calcium acetate. These conditions were optimized by systematically varying each buffer component as well as by adding ligands. The final crystals were produced in the following conditions: 12% PEG 8000, 0.1 M sodium cacodylate, pH 6.5, 0.2 M calcium acetate, and 1 mM Fru-6-P. W179Y/Y164W BsPFK concentration was 7.5 mg/mL.

X-ray diffraction data were collected at room temperature on a Nonius/MAC Science DIP2030 image plate detector using a Rigaku rotating anode as the X-ray source. The data were processed using Denzo and Scalepack to 3.1 Å resolution (27). A clear solution to the molecular replacement was found using the software package "Automated Molecular Replacement" (AMoRe) (28). Refinement of the structure was performed using standard methods as described in "Crystallography and NMR System" (CNS) (29). Noncrystallographic symmetry constraints were used during the refinement. CNS was also used to refine the positions of Fru-6-P and water molecules built into the structure. The final R -factor was 17.87, $R_{\text{free}} = 27.46$, with good stereochemistry.

RESULTS

In simply comparing the kinetic and coupling properties of W179Y/Y164W BsPFK with wild-type BsPFK, there were no dramatic changes observed (Table 1). The specific activity of the mutant is decreased by a factor of 2 compared to wild-type. W179Y/Y164W has a dissociation constant for Fru-6-P, K_{ia}° , of 8.4 \pm 1.5 μM , which is a 3-fold increase in binding affinity compared to wild-type BsPFK. The mutant displays a dissociation constant for PEP, K_{iy}° , of 30.8 \pm 8.0 μM , which is a 2-fold decrease in binding affinity. The coupling parameter, Q_{ay} , which describes the extent of interaction between Fru-6-P bound in the active site and PEP bound in the allosteric site, decreases 2-fold in the mutant

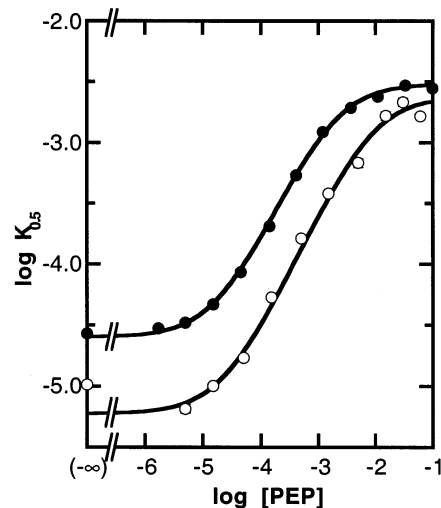


FIGURE 1: Comparison of the coupling interaction between Fru-6-P and PEP for wild-type (●) and W179Y/Y164W (○) BsPFKs. The logarithm of $K_{0.5}$ for Fru-6-P is plotted as a function of the logarithm of PEP concentration for each enzyme. The apparent $K_{0.5}$ for Fru-6-P was determined at each PEP concentration by fitting data obtained from steady-state kinetic experiments to eq 1. The solid line represents the best fit of the data to eq 2. The data were weighted according to the error calculated on the individual $K_{0.5}$ determination. Error bars are plotted and appear smaller than the symbols. MgATP concentration was held constant at 3 mM. Assays were performed at 25 °C and pH 7.0.

Table 2: Steady-State Fluorescence Properties of W179F/F230W and W179Y/Y164W BsPFKs

		W179F/F230W ^a	W179Y/Y164W
Δ intensity	+1 mM Fru-6-P	NC ^b	25% decrease
	+1 mM PEP	35% increase	80% decrease
polarization	no ligands	0.252 \pm 0.001	0.327 \pm 0.001
	+1 mM Fru-6-P	ND ^c	0.353 \pm 0.001
	+1 mM PEP	0.265 \pm 0.001	0.290 \pm 0.001

^a Described previously (16). ^b No change. ^c Not determined.

compared to wild-type. This indicates that PEP is a slightly better inhibitor for the mutant. The observed disparities in the thermodynamic parameters obtained for the mutant and wild-type enzymes are depicted graphically in Figure 1. The difference observed in the coupling parameter, Q_{ay} , between the mutant and wild-type enzymes is essentially due to the increased binding affinity the mutant displays for Fru-6-P in the absence of effector as illustrated by the lower plateaus of the data shown in Figure 1. The upper plateau, which represents the affinity the enzyme displays for Fru-6-P at saturating effector, is nearly identical, indicating that a similar ternary complex is being formed.

W179Y/Y164W BsPFK shows altered fluorescence characteristics compared to wild-type BsPFK. A comparison of the steady-state fluorescence properties of W179Y/Y164W and W179F/F230W (previously described in ref 16) is summarized in Table 2. Fru-6-P binding to W179Y/Y164W causes a 25% decrease in fluorescence intensity and an increase in fluorescence polarization from 0.327 \pm 0.001 to 0.353 \pm 0.001. In contrast, Fru-6-P binding to W179F/F230W causes no observable change in tryptophan fluorescence. PEP binding to W179Y/Y164W produces a dramatic 80% quenching of fluorescence intensity and a decrease in polarization from 0.327 \pm 0.001 to 0.290 \pm 0.001. The changes in fluorescence intensity and polarization associated

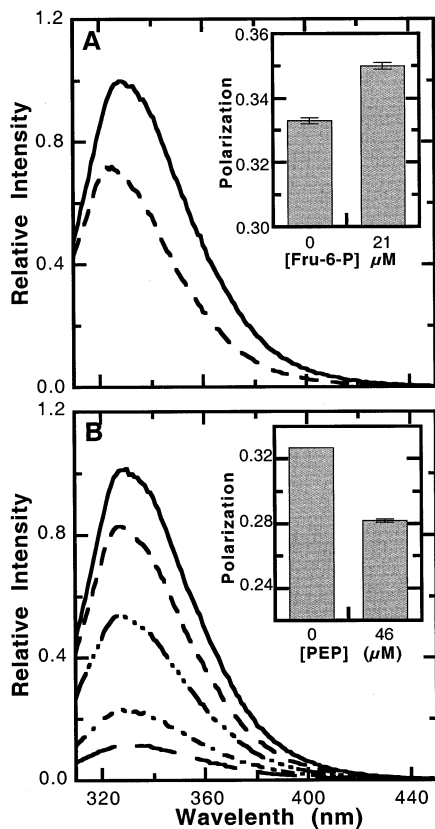


FIGURE 2: Steady-state fluorescence properties of W179Y/Y164W BsPFK in the absence or presence of either Fru-6-P (A) or PEP (B). The concentrations of Fru-6-P shown in (A) were 0 (—) and 21 μM (---). The concentrations of PEP shown in (B) are 0 (—), 5 (---), 10 (— · — · —), 19 (---), and 57 μM (---). The steady-state fluorescence intensity was normalized to protein concentration. Inset figures represent the polarization changes associated with the binding of each ligand, respectively.

with Fru-6-P and PEP binding are illustrated in Figure 2A and 2B, respectively.

As shown in Figure 3, the observed change in fluorescence intensity associated with the addition of PEP yields a binding isotherm. A dissociation constant of $9.4 \pm 0.3 \mu\text{M}$ was measured in the absence of Fru-6-P. The dissociation constant for PEP increases as the fixed concentration of Fru-6-P is increased (Figure 3), which is expected considering the antagonistic relationship between these two ligands. The dissociation constants for PEP measured as a function of Fru-6-P concentration from the series of experiments shown in Figure 3 were used to determine the thermodynamic parameters associated with the binding and the coupling interaction of these ligands as described by eq 2. The parameters derived from the analysis of the data shown in Figure 3 are given in Table 1. The dissociation constant for Fru-6-P, $0.11 \pm 0.04 \mu\text{M}$, is decreased compared to the value determined using kinetic experiments (Table 1). However, as discussed previously, MgATP has an antagonistic effect on the binding affinity for Fru-6-P, causing a greater apparent dissociation constant to be observed in experiments in which MgATP is present, i.e., kinetic assays (30). The dissociation constant for PEP and the coupling parameter are decreased slightly in the fluorescence assays as compared to the kinetic assays.

The large decrease in fluorescence intensity produced by PEP binding suggests that W179Y/Y164W is undergoing a dramatic structural change which significantly alters the

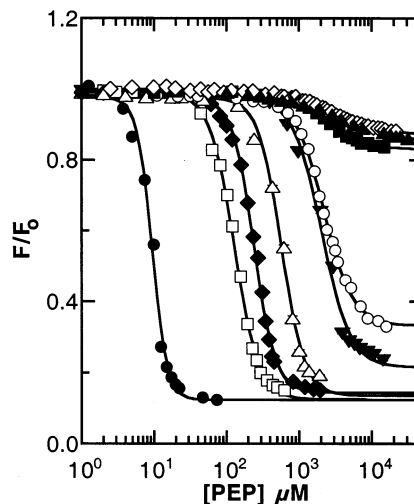


FIGURE 3: Relative fluorescence intensity of W179Y/Y164W BsPFK as a function of PEP concentration at multiple concentrations of Fru-6-P. W179Y/Y164W BsPFK was titrated with PEP at the following Fru-6-P concentrations: 0 (\bullet), 2 (\square), 4 (\blacklozenge), 8 (\triangle), 25 (\blacktriangledown), 40 (\circ), 200 (\blacksquare), 1000 (\diamond), and 5000 μM (\blacktriangle). The solid lines represent the best fit to eq 4. At Fru-6-P concentrations below 200 μM , the binding curves represent PEP binding and dissociation of the enzyme into dimers. Concentrations of Fru-6-P above 200 μM (\blacksquare) appear to stabilize the tetramer even at saturating PEP concentrations, as shown by the diminution of the total change in fluorescence intensity observed at these concentrations.

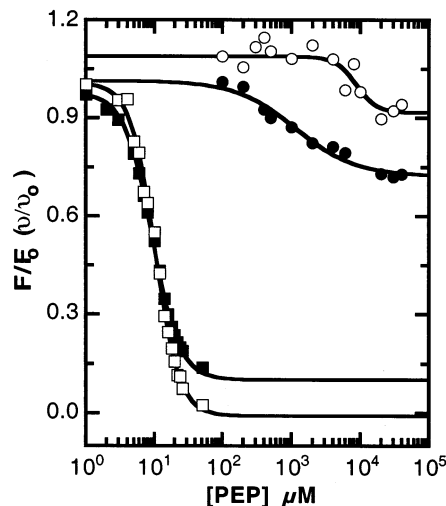


FIGURE 4: Fluorescence intensity and enzyme activity as a function of [PEP]. W179Y/Y164W BsPFK was titrated with PEP in the absence (squares) and presence (circles) of 1 mM Fru-6-P. At each PEP concentration, an aliquot was assayed for enzyme activity (open symbols), and the fluorescence intensity (closed symbols) of the sample was measured. The lines represent the best fit to a modified version of eq 1.

environment of the tryptophan. Upon further examination, PEP binding to W179Y/Y164W was found to cause a complete loss of enzymatic activity which coincides with the decrease in fluorescence intensity as shown in Figure 4. However, incubation of the enzyme with Fru-6-P substantially protects the enzyme from inactivation by PEP. Shown in Figure 4, the effects on both activity and fluorescence intensity caused by PEP binding diminish when the enzyme is incubated with Fru-6-P prior to titration with PEP. At high PEP, even in the presence of Fru-6-P, a relatively small decrease in fluorescence intensity and activity is observed. The notable difference in the transition point between the

intensity and activity data in the presence of Fru-6-P (Figure 4) is most likely due to cooperative processes induced by MgATP which is present at a saturating concentration during the activity measurements.

Two reasonable explanations for the results discussed thus far are as follows: (1) The large fluorescence change caused by PEP binding is a result of a drastic conformational shift in the protein structure such that the local environment of the tryptophan is dramatically altered. This structural change must also distort the active site of the protein in such a way that catalysis can no longer occur. (2) PEP binding causes the enzyme to dissociate into smaller oligomeric species (most likely dimers) which are inactive. There are several empirical observations that support the latter possibility. PEP binds to the enzyme along one subunit interface so it is likely that PEP stabilizes the allosteric site interface. Fru-6-P, however, binds along the active site interface; therefore, dissociation along that interface would lead to a loss of enzymatic activity due to the inability of Fru-6-P to bind. Furthermore, Fru-6-P incubation prior to addition of PEP protects the enzyme from inactivation. Finally, the decrease in fluorescence polarization observed upon PEP binding is consistent with a change in the size of the protein (31). A tetrameric species would most likely have a higher polarization value than a dimeric species assuming the fluorescence lifetime and the local flexibility of the tryptophan remain unchanged.

One way to test the hypotheses rendered above is to determine if PEP-induced inactivation is reversible. As shown by the experiments discussed above, incubation of the enzyme with Fru-6-P prior to addition of PEP protects the enzyme from inactivation. Can the addition of Fru-6-P after inactivation restore activity? W179Y/Y164W BsPFK was incubated at a saturating PEP concentration as determined by fluorescence titration. Inactivation of the enzyme is rapid, and no activity is observed in the first enzymatic assay conducted immediately following addition of PEP. The enzyme is then incubated with a saturating concentration of Fru-6-P, and enzymatic activity assays are performed as a function of time.

If the enzyme were undergoing a large conformational change that rendered the enzyme inactive as a result of PEP binding (hypothesis 1 from above), the rate of reactivation of the enzyme would not be dependent upon enzyme concentration. Conversely, if the enzyme were dissociating into dimers as a result of PEP binding (hypothesis 2 from above), the rate of reactivation would be dependent upon enzyme concentration. As shown in Figure 5, enzymatic activity is recovered by the addition of Fru-6-P. The rate and extent of recovery are dependent upon enzyme concentration. In addition, inactivated enzyme can be incubated with PEP for as long as 24 h before addition of Fru-6-P, and activity can still be recovered (data not shown). By plotting the reciprocal of inactive [PFK] as a function of time (Figure 5 inset), a linear dependence is observed. The rate constant for the dimer to tetramer reassociation reaction can be obtained from the slope of the line and is equal to $6.2 \pm 0.3 \text{ M}^{-1} \text{ s}^{-1}$. Since wild-type BsPFK does not respond to PEP binding in the same way, similar experiments using the native enzyme could not be performed.

To further demonstrate that W179Y/Y164W was undergoing dissociation into dimers and not completely dissociating

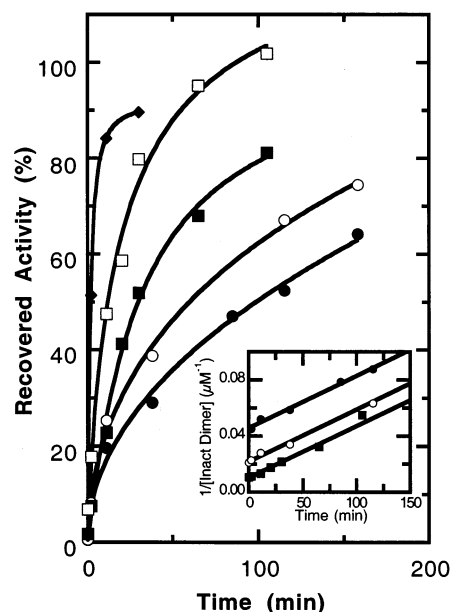


FIGURE 5: Reactivation of W179Y/Y164W BsPFK. Each sample had complete loss of activity within the first minute after addition of PEP. Recovery of activity after the addition of Fru-6-P is represented as percent recovered activity as a function of time. Five different concentrations of W179Y/Y164W are shown: 0.24 (●), 0.48 (○), 0.96 (■), 2.6 (□), and 13.2 μM (◆). Inset: The rate constant for dimer–tetramer association can be obtained from the slope of a plot of reciprocal inactive PFK concentration as a function of time.

into monomers, ultracentrifugation was employed to explicitly determine the molecular weight of the protein in the presence of Fru-6-P and/or PEP. As shown in Figure 6, the data collected for the mutant enzyme, in all cases, could not be fit to a single sedimenting species model. The data obtained for enzyme that had been incubated with Fru-6-P or PEP followed by Fru-6-P fit to a self-associating model, which included a tetramer–dimer equilibrium constant. Under both conditions in which Fru-6-P was present, similar equilibrium constants were obtained, 11.8 ± 0.5 and $12.7 \pm 0.4 \mu\text{M}$, respectively. In the presence of PEP alone, however, the data could not be modeled to a tetramer–dimer equilibrium. Instead these data were fit to a monomer–dimer equilibrium model, and an equilibrium constant of $7.5 \pm 0.02 \mu\text{M}$ was calculated.

The unique response that W179Y/Y164W has with regard to PEP binding raises some question concerning the structure of the mutant enzyme. Specifically, have the mutations caused a large structural change within the protein that is responsible for the observed effects? Diffraction quality crystals of W179Y/Y164W with Fru-6-P bound were obtained. The crystals belonged to space group $P2_1$ with unit cell dimensions of 110.7 Å, 106.9 Å, and 119.6 Å. There were 8 subunits (two tetramers) per asymmetric unit. A total of 19 328 non-hydrogen atoms were observed. The details regarding the diffraction data and refinement statistics are given in Table 3.

An overlay of the structure obtained for W179Y/Y164W and wild-type BsPFK (6) in the area of residue 164 and Fru-6-P and residue 179 is shown in Figure 7. Residues within the active and allosteric site that have been proposed to be important for ligand binding as well as the residues at positions 164 and 179 are shown in each of the overlaid

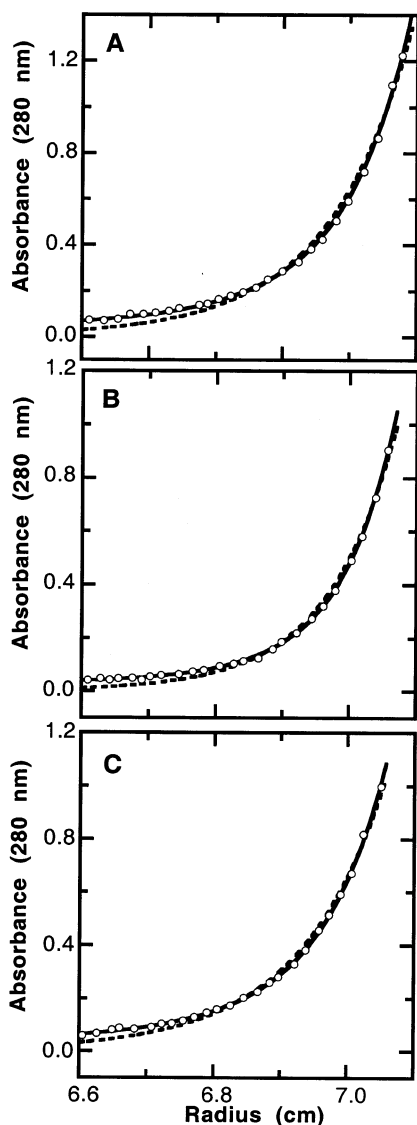


FIGURE 6: Ultracentrifugation traces for W179Y/Y164W in the presence of Fru-6-P (A), PEP (B), and PEP and Fru-6-P (C). Samples were prepared as described under Materials and Methods. The solid line represents the best fit to the data using an associated species model (eq 6). The dashed line represents simulated data for a single sedimenting species in solution, which would be a tetramer in the case of (A) and (C) or a dimer in the case of (B). For clarity in the presentation, the data points are a representative sampling of the data actually collected and used for analysis.

structures. No major structural differences between the mutant and wild-type enzymes with Fru-6-P bound are evident. Unfortunately, attempts to obtain crystal of W179Y/Y164W in the presence of PEP have not been successful, so it is difficult to say what effects PEP may have on the global structure of the protein.

DISCUSSION

Many studies have been conducted comparing the structures of enzymes from mesophilic and thermophilic sources in order to deduce structural features of thermophilic enzymes that confer thermal stability (32–37). Some of the common stabilizing features found in thermophilic enzymes are an increased number of salt bridges, additional hydrogen bonds, higher percentage of proline residues, and a more hydrophobic subunit interface, just to name a few (33, 34). Not

Table 3: Diffraction and Refinement Statistics for Crystallization of W179Y/Y164W BsPFK

Diffraction Data	
parameter	value
resolution (Å)	3.1
completeness (%) (total/highest) ^a	91.6/89.7
no. of reflections (total/unique)	106908/46829
I/σ	7.6
R_{sym}^b (%)	10.1
Refinement Statistics	
parameter	value
reflections in working set	32894
R_{cryst} (%)	17.87
R_{free} (%)	27.46
rmsd bond lengths (Å)	0.008
rmsd bond angles (deg)	1.146
average B factor (Å ²)	41.70

^a Highest resolution shell. ^b $R_{\text{sym}} = \sum |I - \langle I \rangle| / \sum \langle I \rangle$, where I is the observed intensity and $\langle I \rangle$ is the average intensity of multiple observations of symmetry-related reflections.

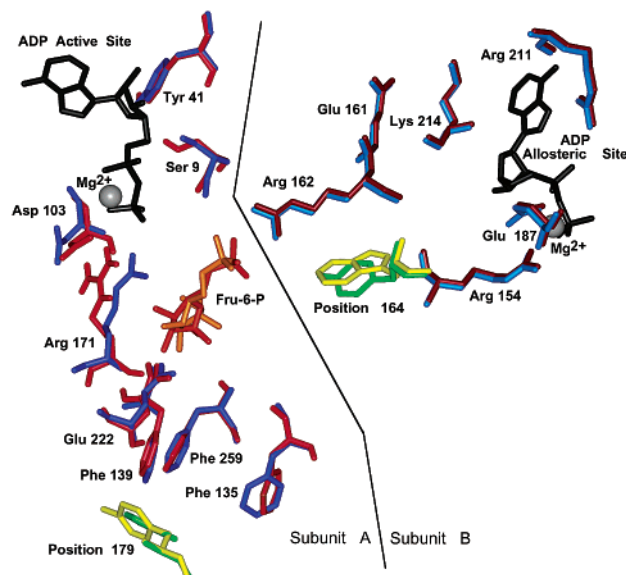


FIGURE 7: Crystal structures of wild-type and W179Y/Y164W BsPFK. The structures have been overlaid, and select residues within the active and allosteric site are shown. ADP bound in either the active site or the allosteric site is shown in black, Fru-6-P bound in the active site is shown in orange, and magnesium ions bound in both the active and allosteric sites are shown as gray spheres. MgADP is present in the active and allosteric site of the wild-type structure only. The red residues represent the wild-type structure while the blue residues are from W179Y/Y164 mutant structure. The different shades of either red or blue indicate residues from different subunits. Highlighted in green are the tryptophan (position 179) and the tyrosine (position 164) in the wild-type structure, and highlighted in yellow are the tyrosine (position 179) and the tryptophan (position 164) in the mutant structure. The crystal structure for W179Y/Y164W was obtained as described under Materials and Methods. The crystal structure for wild-type BsPFK was adapted from the structure designated PDB 4PFK obtained from the Protein DataBank (31). Structures were examined and modified using InsightII Version 98.0 Molecular Modeling System (Molecular Simulations, Inc., San Diego, CA).

all of these stabilizing factors are apparent in all thermophilic enzymes. Usually each enzyme has a unique combination of stabilizing features which render it stable at elevated temperatures.

One of the most common features of thermophilic enzymes is that their structure is relatively rigid (15, 33, 34, 37). This

means that the allosteric response of thermophilic enzymes may be different than their mesophilic counterparts which have a larger degree of conformational flexibility. One example, in particular, is PFK from *Thermus thermophilus* (TtPFK). TtPFK is reported to dissociate from active tetramers to inactive dimers in response to allosteric ligand binding (4). In another example, BsPFK, a dimer of rigid dimers, undergoes a 7° rotation of the dimers relative to one another in response to PEP binding (38). Although the allosteric properties of thermophilic enzymes have not been as extensively studied as their mesophilic counterparts, from the above-mentioned structural studies it seems likely that the oligomeric interactions play a substantial role in the allosteric response of enzymes from thermophilic sources.

The experiments discussed in this study have clearly shown that W179Y/Y164W BsPFK undergoes reversible dissociation along the active site interface in response to PEP binding in the allosteric site. Even though this phenomenon is not observed with the wild-type enzyme, these data suggest that quaternary structural changes along interfaces may play an important role in the allosteric effect. The position of Tyr164 is approximately 6 Å from the Fru-6-P binding site across the active site interface (6, 38, 39). The crystal structure of W179Y/Y164W BsPFK in the presence of Fru-6-P does not show major structural changes at the interface; however, the destabilization occurs in response to PEP binding in the allosteric site. Unfortunately, crystallization attempts of this mutant in the presence of PEP have been unsuccessful.

The kinetic properties of W179Y/Y164W BsPFK are not drastically altered compared to the wild-type enzyme. The dissociation constant for Fru-6-P is not compromised by the mutations; in fact, the mutant displays a $K_{0.5}$ value for Fru-6-P that is one-third that of the wild-type enzyme. The activity of the enzyme is decreased by 50% compared to the wild-type enzyme. These results suggest that the binding site of the mutant enzyme may be altered slightly, but there are no obvious changes observed in the crystal structure (Figure 7). One possible explanation for the decreased activity is that the tetramer-dimer equilibrium for the mutant is altered compared to the wild-type enzyme even in the absence of ligands. Considering the behavior of the mutant enzyme with regard to PEP binding, it is remarkable that the coupling between Fru-6-P and PEP is not dramatically affected by the mutations. The difference in Q_{ay} between the mutant and wild-type enzymes appears to be due to the altered binding affinity the mutant displays for Fru-6-P (Figure 1) in the absence of inhibitor.

A better understanding of the role of subunit interactions in the allosteric response of thermophilic enzymes may be revealed by a comparison of the thermal stability and allosteric properties of EcPFK, wild-type and W179Y/Y164W BsPFK, and TtPFK.

REFERENCES

- Uyeda, K. (1979) *Adv. Enzymol. Relat. Areas Mol. Biol.* 48, 193–224.
- Blangy, D., Buc, H., and Monod, J. (1968) *J. Mol. Biol.* 31, 13–35.
- Hengartner, H., and Harris, J. I. (1975) *FEBS Lett.* 55, 282–285.
- Xu, J., Oshima, T., and Yoshida, M. (1990) *J. Mol. Biol.* 215, 597–606.
- Parmeggiani, A., Luft, J. H., Love, D. S., and Krebs, E. G. (1966) *J. Biol. Chem.* 241, 4625–4637.
- Evans, P. R., and Hudson, P. J. (1979) *Nature* 279, 500–504.
- Ling, K. H., Marcus, F., and Lardy, H. A. (1965) *J. Biol. Chem.* 240, 1893–1899.
- Reinhart, G. D., and Lardy, H. A. (1980) *Biochemistry* 19, 1477–1484.
- Reinhart, G. D., and Lardy, H. A. (1980) *Biochemistry* 19, 1484–1490.
- Reinhart, G. D., and Lardy, H. A. (1980) *Biochemistry* 19, 1491–1495.
- Xu, J., Seki, M., Denda, K., and Yoshida, M. (1991) *Biochem. Biophys. Res. Commun.* 176, 1313–1318.
- Drozdov-Tikhomirov, L. N., Skurida, G. I., and Alexandrov, A. A. (1999) *J. Biomol. Struct. Dyn.* 16, 917–929.
- Johnson, J. L., and Reinhart, G. D. (1994) *Biochemistry* 33, 2635–2643.
- Johnson, J. L., and Reinhart, G. D. (1997) *Biochemistry* 36, 12814–12822.
- Kim, S. J., Chowdhury, F. N., Stryjewski, W., Younathan, E. S., Russo, P. S., and Barkley, M. D. (1993) *Biophys. J.* 65, 215–226.
- Riley-Lovingshimer, M., and Reinhart, G. D. (2001) *Biochemistry* 40, 3002–3008.
- Pace, C. N., Vajdos, J., Fee, L., Grimsley, G., and Gray, T. (1995) *Protein Sci.* 4, 2411–2423.
- Babul, J. (1978) *J. Biol. Chem.* 253, 4350–4355.
- Kotlarz, D., and Buc, H. (1982) *Methods Enzymol.* 90, 60–70.
- Hill, A. V. (1910) *J. Physiol. (London)* 40, iv–vii.
- Braxton, B. L., Tlapak-Simmons, V. L., and Reinhart, G. D. (1994) *J. Biol. Chem.* 269, 47–50.
- Tlapak-Simmons, V. L., and Reinhart, G. D. (1994) *Arch. Biochem. Biophys.* 308, 226–230.
- Tlapak-Simmons, V. L., and Reinhart, G. D. (1998) *Biophys. J.* 75, 1010–1015.
- Johnson, M. L., Correia, D. A., Yphantis, D. A., and Halvorson, H. R. (1981) *Biophys. J.* 36, 575–588.
- McRorie, D. K., and Voelker, P. J. (1993) Beckman Instruments, Inc., Fullerton, CA.
- Voelker, P. J., and McRorie, D. K. (1993) Beckman Instruments, Inc., Fullerton, CA.
- Otwinowski, Z., and Minor, W. (1997) *Methods Enzymol.* 276, 307–326.
- Navaza, J. (1994) *Acta Crystallogr. A* 50, 157–163.
- Brunger, A. T., Adams, P. D., Clore, G. M., DeLano, W. L., Gros, P. R., Grosse-Kunstleve, W., Jiang, J. S., Kuszewski, J., Nilges, M., Pannu, N. S., Read, R. J., Rice, L. M., Simonson, T., and Warren, G. L. (1998) *Acta Crystallogr. D* 54, 905–921.
- Byrnes, M., Xhu, X., Younathan, E. S., and Chang, S. H. (1994) *Biochemistry* 33, 3424–3431.
- Lakowicz, J. R. (1999) *Principles of Fluorescence Spectroscopy*, 2nd ed., Plenum, New York.
- Kirino, H., Aoki, M., Aoshima, M., Hayashi, Y., Ohba, M., Yamagishi, A., Wakagi, T., and Oshima, T. (1994) *Eur. J. Biochem.* 220, 275–281.
- Salminen, T., Teplyakov, A., Kankare, J., Cooperman, B. S., Lahti, R., and Goldman, A. (1996) *Protein Sci.* 5, 1014–1025.
- Wallon, G., Kryger, G., Lovett, S. T., Oshima, T., Ringe, D., and Petsko, G. A. (1997) *J. Mol. Biol.* 266, 1016–1031.
- Auerbach, G., Ostendorp, R., Prade, L., Korndorfer, I., Dams, T., Huber, R., and Jaenicke, R. (1998) *Structure* 6, 769–781.
- Hansen, T., Urbanke, C., Leppanen, V. M., Goldman, A., Brandenburg, K., and Schafer, G. (1999) *Arch. Biochem. Biophys.* 363, 135–147.
- Hollien, J., and Marqusee, S. (1999) *Biochemistry* 38, 3831–3836.
- Schirmer, T., and Evans, P. R. (1990) *Nature* 343, 140–145.
- Evans, P. R., Farrants, G. W., and Hudson, P. J. (1981) *Philos. Trans. R. Soc. London B* 293, 83–62.